Cancer Science

WILEY

Cancer Science

ORIGINAL ARTICLE OPEN ACCESS

Antitumor Activities by a Humanized Cancer-Specific Anti-Podoplanin Monoclonal Antibody humPMab-117 Against Human Tumors

Tomohiro Tanaka[1] | Hiroyuki Suzuki[1] | Tomokazu Ohishi[2] | Manabu Kawada[2] | Mika K. Kaneko[1] | Yukinari Kato[1]

[1]Department of Antibody Drug Development, Tohoku University Graduate School of Medicine, Sendai, Japan | [2]Laboratory of Oncology, Institute of Microbial Chemistry (BIKAKEN), Microbial Chemistry Research Foundation, Shinagawa-ku, Japan

Correspondence: Hiroyuki Suzuki (hiroyuki.suzuki.b4@tohoku.ac.jp) | Yukinari Kato (yukinari.kato.e6@tohoku.ac.jp)

Received: 21 March 2025 | **Revised:** 3 May 2025 | **Accepted:** 7 May 2025

Funding: This research was supported in part by the Japan Agency for Medical Research and Development (AMED) (Grants JP24am0521010 [to Y.K.], JP24ama121008 [to Y.K.], JP24ama221339 [to Y.K.], JP24bm1123027 [to Y.K.], and JP24ck0106730 [to Y.K.]), and by the Japan Society for the Promotion of Science (JSPS) Grants-in-Aid for Scientific Research (KAKENHI) (Grants 22K06995 [to H.S], 24K18268 [to T.T.], and 22K07224 [to Y.K.]).

Keywords: ADCC | antitumor activity | cancer-specific monoclonal antibody | CDC | podoplanin

ABSTRACT

Podoplanin (PDPN), also referred to as T1α/Aggrus, is a type I transmembrane sialoglycoprotein that plays a crucial role in invasiveness, stemness, and epithelial-to-mesenchymal transition, all of which contribute to the malignant progression of tumors. Therefore, a monoclonal antibody (mAb) against PDPN has been evaluated in preclinical models as a promising tumor therapy strategy. However, PDPN plays an essential role in normal development, such as in the development of the lungs. On-target toxicity by anti-PDPN mAbs to normal cells should be avoided to minimize adverse effects. A cancer-specific mAb against PDPN, PMab-117 (rat IgM, kappa), was previously established. This study engineered the humanized IgG_1 version (humPMab-117) to investigate antitumor activity. Flow cytometry analysis confirmed that humPMab-117 recognized PDPN-overexpressed glioma LN229 (LN229/PDPN) cells as well as PDPN-positive PC-10 (human lung squamous cell carcinoma) and LN319 (human glioblastoma) cells. In contrast, humPMab-117 did not react with normal epithelial cells from the lung bronchus, gingiva, mammary gland, corneal, and normal kidney podocytes, suggesting that humPMab-117 retains cancer-specific reactivity. Furthermore, humPMab-117 effectively induced antibody-dependent cellular cytotoxicity and complement-dependent cytotoxicity against LN229/PDPN, PC-10, and LN319 cells. In the xenograft tumor models, humPMab-117 demonstrated strong antitumor efficacy. These results suggest the potential of humPMab-117 as a therapeutic antibody for treating PDPN-positive malignant tumors.

Abbreviations: ADCC, antibody-dependent cellular cytotoxicity; CAR-T, chimeric antigen receptor-T; CasMab, cancer-specific monoclonal antibody; CDC, complement-dependent cytotoxicity; CDR, complementarity-determining region; CLEC-2, C-type lectin-like receptor 2; HER2, human epidermal growth factor receptor 2; mAb, monoclonal antibody; NK cells, natural killer cells; PDPN, podoplanin; PLAG, platelet aggregation-stimulating; PLD, PLAG-like domain; SCC, squamous cell carcinoma.

Tomohiro Tanaka, Hiroyuki Suzuki, and Tomokazu Ohishi contributed equally to this article.

1 | Introduction

The validation of adequate antigenic targets is essential for the development of monoclonal antibody (mAb)-based tumor therapy [1]. To achieve an acceptable therapeutic index with low on-target toxicity, targets highly expressed in tumors and little or no expression in normal tissues are considered ideal antigenic targets. However, the number of ideal antigenic targets is limited, which is a significant problem for developing therapeutic mAbs for tumors.

To solve the problem, we have developed cancer-specific mAbs (CasMabs) for various antigens and revealed the cancer-specific epitope and the recognition structure. In the anti-humanepidermal growth factor receptor 2 (HER2) CasMab development, we established more than 300 anti-HER2 mAb clones by immunization of mice with cancer cell-expressed HER2. These mAbs were screened by the reactivity to HER2-expressed tumor and normal cells by flow cytometry [2]. Among them, H_2Mab-250/H_2CasMab-2 recognized HER2 in breast cancer cells but not in normal epithelial cells from the mammary gland, lung bronchus, colon, and kidney proximal tubule [2]. Epitope analysis identified Trp614 in the extracellular domain 4 of HER2 as a critical residue for H_2Mab-250 recognition [2].

Furthermore, mouse IgG_{2a} type or humanized H_2Mab-250 exhibited antibody-dependent cellular cytotoxicity (ADCC), complement-dependent cytotoxicity (CDC), and in vivo antitumor efficacy against human breast cancer xenografts [3–5]. A single chain variable fragment of H_2Mab-250 was further developed to chimeric antigen receptor (CAR)-T cell therapy and showed cancer-specific recognition and cytotoxicity [6]. A phase I clinical trial is underway for patients with HER2-positive advanced solid tumors in the US (NCT06241456). Therefore, selecting CasMab and identifying the cancer-specific epitopes are essential strategies for developing therapeutic mAbs and modalities.

Podoplanin (PDPN) (also known as T1α, PA2.26 antigen, E11 antigen, and Aggrus) is a heavily glycosylated type I transmembrane protein, which has an N-terminal extracellular domain, a transmembrane domain, and a short intracellular domain [7, 8]. The N-terminal extracellular domain possesses platelet aggregation-stimulating (PLAG) domains, which have a consensus repeat sequence of EDxxVTPG [9]. The *O*-glycosylation sites at Thr52 in PLAG3 or a PLAG-like domain (PLD, also named PLAG4) have been reported to be crucial for the interaction of PDPN to C-type lectin-like receptor 2 (CLEC-2), which is essential for platelet aggregation and hematogenous metastasis to lung [10, 11].

PDPN is involved in the malignant progression of tumors by promoting invasiveness and metastasis. PDPN-expressing tumor cells show a diverse pattern of invasion [12], including the epithelial-to-mesenchymal transition-like pattern in various tumors [13, 14], collective invasion in squamous cell carcinomas (SCCs) [15], and ameboid invasion in melanoma [16]. The intracellular domain of PDPN possesses basic residues as binding sites for ezrin, radixin, and moesin proteins [17], which mediate Rho GTPase activity and regulate the diverse pattern of invasiveness [18, 19]. Furthermore, PDPN binds to matrix metalloproteinases [20] and a hyaluronan receptor CD44 [21], which mediate the invadopodia formation and extracellular matrix degradation. In the clinic, high PDPN expression was associated with shortened overall survival in patients with gliomas, head and neck SCC, esophageal SCC, gastric adenocarcinomas, and mesotheliomas [22–25]. Therefore, PDPN has been considered a promising target of mAb-based therapy. However, PDPN also plays an essential role in normal cells, such as lung alveolar type I cells [26] and kidney podocytes [27, 28]. Therefore, cancer-specific reactivity is required to reduce adverse effects on normal cells.

We have developed CasMabs against PDPN by selecting the cancer-specific reactivity in flow cytometry and immunohistochemistry. LpMab-2 [29] and LpMab-23 [30] were obtained by immunization of mice with PDPN-overexpressed glioblastoma LN229 (LN229/PDPN). LpMab-2 recognizes a glycopeptide structure (Thr55-Leu64) of PDPN [29]. In contrast, LpMab-23 recognizes a naked peptide structure (Gly54-Leu64) of PDPN [31]. Mouse-human chimeric LpMab-2 and LpMab-23 (chLpMab-2 and chLpMab-23, respectively) exhibited the ADCC activity and antitumor effect in human tumor xenograft models [31, 32]. Furthermore, we obtained another CasMab against PDPN (PMab-117) by immunization of a rat with LN229/PDPN. In flow cytometry, PMab-117 showed reactivity to PDPN-expressing tumor PC-10 and LN319. PMab-117 did not react with normal kidney podocytes and epithelial cells from the mammary gland, lung bronchus, and cornea. In contrast, NZ-1, one of the non-CasMabs against PDPN, exhibited high reactivity to both tumor and normal cells [33]. PMab-117 recognizes the glycopeptide structure of PDPN (Ile78-Thr85) within PLD, including *O*-glycosylated Thr85 [7].

This study evaluates the effects of the humanized version of PMab-117 (humPMab-117) on the ADCC, CDC, and antitumor activity.

2 | Materials and Methods

2.1 | Cell Lines

PODO/TERT256 and hTCEpi were purchased from EVERCYTE (Vienna, Austria). LN229, HBEC3-KT, hTERT-HME1, and hTERT TIGKs were purchased from the American Type Culture Collection (ATCC, Manassas, VA). Human glioblastoma LN319 cells were purchased from Addexbio Technologies (San Diego, CA, USA). Human lung SCC PC-10 cells were purchased from Immuno-Biological Laboratories Co. Ltd. (Gunma, Japan).

LN229/PDPN cells were established as previously described [29]. LN229, LN229/PDPN, and LN319 cells were cultured in Dulbecco's Modified Eagle's Medium (DMEM) (Nacalai Tesque Inc. [Nacalai], Kyoto, Japan). PC-10 cells were cultured in Roswell Park Memorial Institute-1640 medium (Nacalai). These media were supplemented with 10% heat-inactivated fetal bovine serum (FBS; Thermo Fisher Scientific Inc. [Thermo], Waltham, MA, USA), 0.25 μg/mL amphotericin B, 100 μg/mL streptomycin, and 100 units/mL penicillin (Nacalai). ExpiCHO-S and Fut8-deficient ExpiCHO-S (BINDS-09) cells were cultured as described previously [34].

Immortalized normal epithelial cell lines were maintained as follows: PODO/TERT256, MCDB131 (Pan Biotech, Bayern, Germany) supplemented with GlutaMAX-I (Thermo), Bovine Brain Extract (9.6 μg/mL, Lonza, Basel, Switzerland), EGF (8 ng/mL, Sigma-Aldrich Corp. [Sigma], St. Louis, MO, USA), Hydrocortisone (20 ng/mL, Sigma), 20% FBS (Sigma), and G418 (100 μg/mL, InvivoGen, San Diego, CA); HBEC3-KT, Airway Epithelial Cell Basal Medium and Bronchial Epithelial Cell Growth Kit (ATCC); hTERT TIGKs, Dermal Cell Basal Medium and Keratinocyte Growth Kit (ATCC); hTERT-HME1, Mammary Epithelial Cell Basal Medium BulletKit without GA-1000 (Lonza); hTCEpi, KGMTM-2 BulletKit (Lonza).

All cell lines were cultured at 37°C in a humidified atmosphere with 5% CO_2 and 95% air.

2.2 | Animals

The Institutional Animal Ethics Committee of the Institute of Microbial Chemistry (Tokyo, Japan) authorized animal studies evaluating the antitumor efficacy of humPMab-117 (approval number: 2024-076). The animal studies followed the institutional guidelines from the Animal Ethics Committee of the Institute of Microbial Chemistry. Humane objectives for euthanasia were established as a loss of original body weight to a point > 25% and/or a maximal tumor size > 3000 mm^3.

2.3 | Antibodies

To generate a humanized antihuman PDPN mAb (humPMab-117), the complemantarity-determing regions (CDRs) of PMab-117 V_H, the frame sequence of V_H in human Ig, and the CH of human IgG_1 were cloned into the pCAG-Neo vector. The CDR of PMab-117 V_L, the frame sequence of V_L in human Ig, and the C_L of the human kappa chain were cloned into the pCAG-Ble vector [35]. We transfected the antibody expression vectors of humPMab-117 into BINDS-09 (fucosyltransferase 8-knockout ExpiCHO-S) cells using the ExpiCHO-S Expression System (Thermo). As a control human IgG_1 mAb, humCvMab-62 was produced from CvMab-62 (an anti-SARS-CoV-2 spike protein S2 subunit mAb) using the abovementioned method. NZ-16, a rat-human chimeric anti-PDPN mAb, was previously described [36]. humCvMab-62, humPMab-117, and NZ-16 were purified using Ab-Capcher (ProteNova Co. Ltd., Kagawa, Japan). To confirm the purity of mAbs, they were treated with sodium dodecyl sulfate sample buffer containing 2-mercaptoethanol, separated on 5%–20% polyacrylamide gel (FUJIFILM Wako Pure Chemical Corporation, Osaka, Japan), and stained with Bio-Safe CBB G-250 (Bio-Rad Laboratories Inc., Berkeley, CA).

2.4 | Flow Cytometry

Cells were harvested using 0.25% trypsin and 1 mM ethylenediaminetetraacetic acid (Nacalai). Subsequently, they were washed with 0.1% bovine serum albumin (Nacalai) in phosphate-buffered saline (PBS), followed by treatment with humPMab-117 or NZ-16 for 30 min at 4°C. Then, the cells were treated with fluorescein isothiocyanate-conjugated anti-human IgG (1:2000; Sigma) for 30 min at 4°C. Fluorescence data were collected using the SA3800 Cell Analyzer (Sony Corp., Tokyo, Japan) and analyzed with FlowJo software (BD Biosciences, Franklin Lakes, NJ, USA).

2.5 | Antibody-Dependent Cellular Cytotoxicity

Human natural killer (NK) cells were purchased from Takara Bio Inc. (Shiga, Japan) and were used as effector cells immediately after thawing as follows. Target cells (LN229/PDPN, PC-10, and LN319) were labeled with 10 μg/mL of Calcein AM (Thermo). The target cells were plated in 96-well plates at a density of 5×10^3 cells/well and combined with effector cells (effector-to-target ratio, 50:1) and 100 μg/mL of either control human IgG_1 or humPMab-117. After incubating for 4.5 h, the calcein released into the supernatant was measured as described previously [4].

2.6 | Complement-Dependent Cytotoxicity

The target cells labeled with Calcein AM (LN229/PDPN, PC-10, and LN319) were seeded and combined with rabbit complement (final concentration 10%, Low-Tox-M Rabbit Complement; Cedarlane Laboratories, Hornby, ON, Canada) along with 100 μg/mL of either control human IgG_1 or humPMab-117. After a 4.5-h incubation at 37°C, the amount of calcein released into the medium was measured as described previously [4].

2.7 | Antitumor Activities of humPMab-117 in Xenografts of Human Tumors

LN229/PDPN, PC-10, and LN319 were mixed with DMEM and Matrigel Matrix Growth Factor Reduced (BD Biosciences). Subcutaneous injections were then given to the left flanks of BALB/c nude mice. On the eighth post-inoculation day, 100 μg of control human IgG_1 ($n = 8$) or humPMab-117 ($n = 8$) in 100 μL PBS were administered intraperitoneally. Additional antibody injections were given on days 15 and 22. The tumor diameter was assessed on days 8, 15, 17, 22, and 25 after the tumor cell implantation. Tumor volumes were calculated in the same manner as previously stated. The weight of the mice was also assessed on days 8, 11, 15, 17, 22, and 25 following the tumor cell inoculation. When the observations were finished on day 25, the mice were sacrificed, and tumor weights were assessed following tumor excision.

2.8 | Statistical Analyses

All data are represented as mean ± standard error of the mean (SEM). A two-tailed unpaired *t* test was conducted to measure ADCC activity, CDC activity, and tumor weight. ANOVA with Sidak's post hoc test was performed for tumor volume and mouse weight. GraphPad Prism 8 (GraphPad Software Inc., La Jolla, CA, USA) was used for all calculations. $p < 0.05$ was considered to indicate a statistically significant difference.

3 | Results

3.1 | Production of Humanized Anti-PDPN mAb, humPMab-117

To obtain anti-PDPN CasMabs, we established more than 100 anti-PDPN mAbs by immunization of mice or rats with PDPN-overexpressed tumor cells. These mAbs were screened for reactivity to PDPN-expressed tumor and normal cells by flow cytometry. Among them, an anti-PDPN CasMab (PMab-117; rat IgM, kappa) was established by immunization of LN229/PDPN. PMab-117 was shown to recognize cancer cell-expressed PDPN, but not normal cell-expressed PDPN in flow cytometry [33]. In this study, we engineered a humanized PMab-117 (humPMab-117) by fusing the V_H and V_L CDRs of PMab-117 with the C_H and C_L chains of human IgG_1, respectively (Figure 1A). Under reduced conditions, we confirmed the purity of original and recombinant mAbs by SDS-PAGE (Figure 1B).

As shown in Figure 2A, humPMab-117 reacted with LN229/PDPN, PC-10, and LN319, but not with PDPN-negative LN229 and PDPN-knockout LN319 (BINDS-55). NZ-16, a rat-human chimeric anti-PDPN mAb [36], showed a higher reactivity to those cancer cell lines. We next compared the reactivity of humPMab-117 and NZ-16 to a TERT-expressed normal kidney podocyte, PODO/TERT256, and TERT-expressed normal epithelial cell lines, HBEC3-KT (lung bronchus), hTERT-TIGKs (gingiva), hTERT-HME1 (mammary gland), and hTCEpi (cornea). As shown in Figure 2B, humPMab-117 did not show reactivity to PODO/TERT256, HBEC3-KT, hTERT-TIGKs, hTERT-HME1, and hTCEpi. In contrast, NZ-16 showed reactivity to those normal cells. These results indicated that humPMab-117 retains cancer-specific reactivity.

The K_D values for the interaction of humPMab-117 and NZ-16 with LN229/PDPN were determined by flow cytometry. The K_D values for humPMab-117 and NZ-16 with LN229/PDPN cells were 5.4×10^{-7} M and 8.6×10^{-9} M, respectively (Figure 3). These results indicated that humPMab-117 possesses approximately 60-fold lower affinity to LN229/PDPN than NZ-16.

3.2 | ADCC by humPMab-117 Against PDPN-Positive Cells

We next investigated whether humPMab-117 exhibits ADCC activity against PDPN-positive cells. As shown in Figure 4, humPMab-117 induced significant ADCC against LN229/PDPN cells (18.7% cytotoxicity; $p < 0.05$) compared to the control human IgG_1 (9.8% cytotoxicity). Furthermore, humPMab-117 elicited ADCC against endogenous PDPN-expressing tumor PC-10 (23.4% cytotoxicity; $p < 0.05$) more effectively than the control human IgG_1 (13.0% cytotoxicity). Additionally, humPMab-117 also showed ADCC against endogenous PDPN-expressing tumor LN319 (4.5% cytotoxicity; $p < 0.05$) more effectively than the control human IgG_1 (2.4% cytotoxicity).

3.3 | CDC by humPMab-117 Against PDPN-Positive Cells

We next examined the CDC activity of humPMab-117 against PDPN-positive cells. As shown in Figure 5, humPMab-117 induced significant CDC against LN229/PDPN cells (25.1% cytotoxicity; $p < 0.01$) compared to the control human IgG_1 (4.5% cytotoxicity). Furthermore, humPMab-117 elicited CDC against PC-10 (17.2% cytotoxicity; $p < 0.05$) more effectively than the control human IgG_1 (5.8% cytotoxicity). In addition, humPMab-117

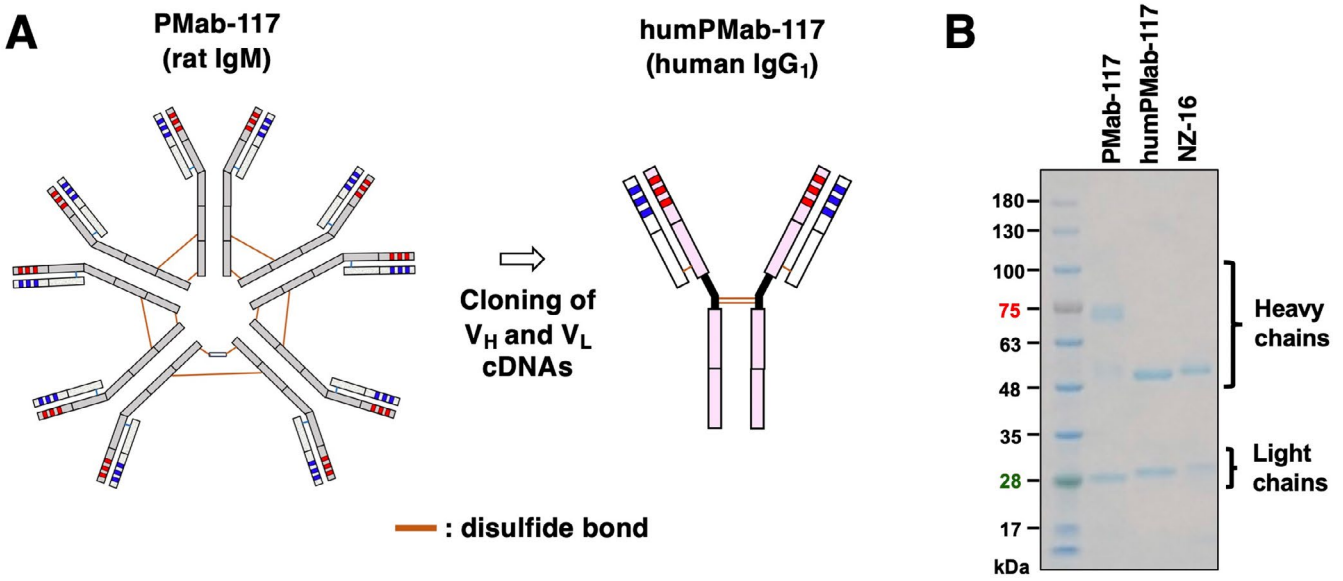

FIGURE 1 | Production of humPMab-117. (A) Human IgG_1 mAb, humPMab-117, was generated from PMab-117 (rat IgM). (B) MAbs were treated with sodium dodecyl sulfate sample buffer containing 2-mercaptoethanol. Proteins were separated on polyacrylamide gel. Bio-Safe CBB G-250 Stain stained the gel.

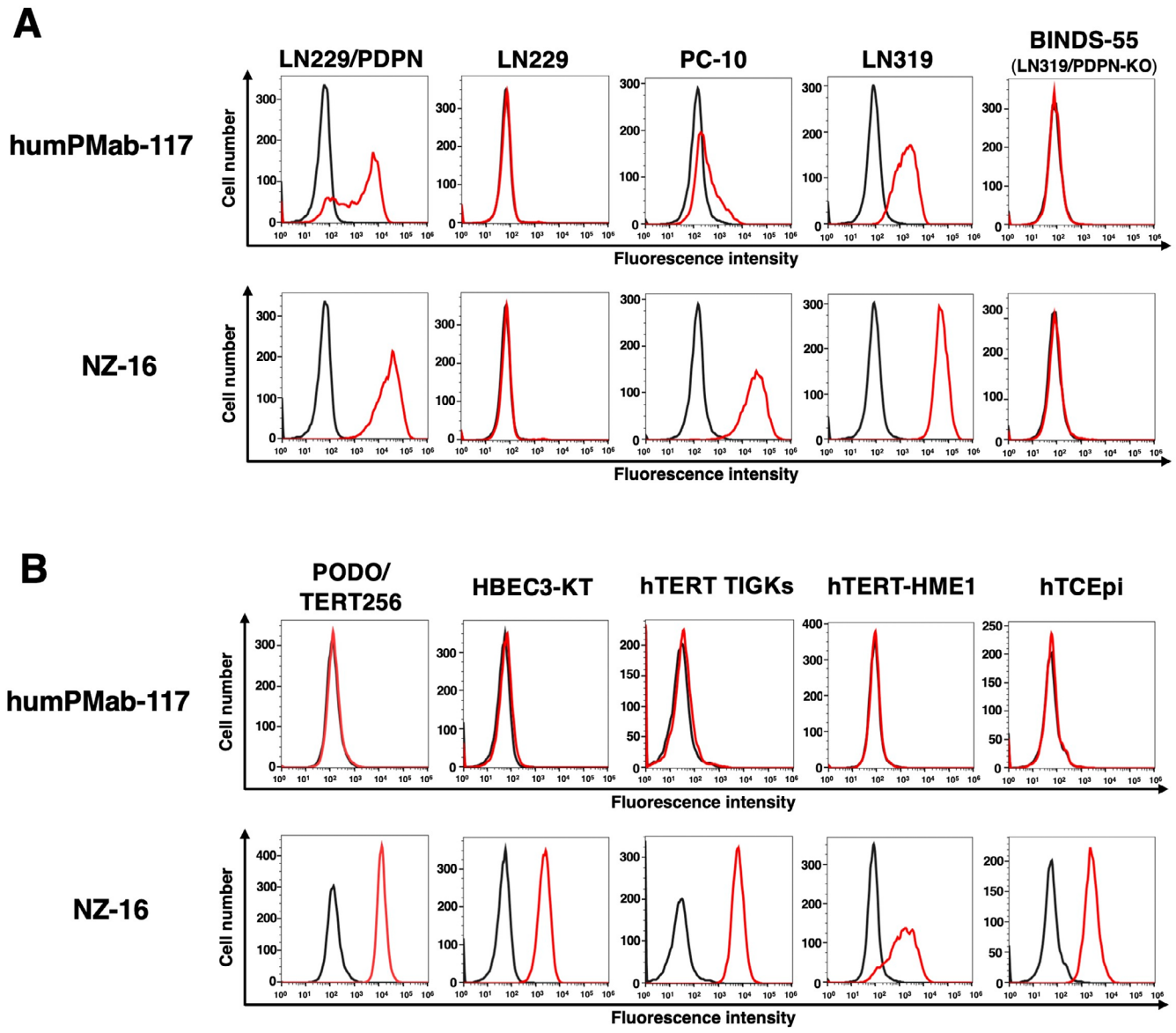

FIGURE 2 | Reactivity of humPMab-117 to cancer cells, normal kidney podocytes, and epithelial cells. (A) Flow cytometry using humPMab-117 (10 μg/mL; Red line), NZ-16 (10 μg/mL; Red line), or buffer control (Black line) against LN229, LN229/PDPN, PC-10, LN319, and PDPN-knockout LN319 (BINDS-55). (B) Flow cytometry using humPMab-117 (10 μg/mL; Red line), NZ-16 (10 μg/mL; Red line) or buffer control (Black line) against PODO/TERT256 (kidney podocyte), HBEC3-KT (lung bronchus epithelial cell), hTERT-TIGKs (gingiva), hTERT-HME1 (mammary gland epithelial cell), and hTCEpi (corneal epithelial cell). The cells were treated with FITC-conjugated antihuman IgG. Fluorescence data were analyzed using the SA3800 Cell Analyzer.

also showed CDC against LN319 (6.6% cytotoxicity; $p < 0.05$) more effectively than the control human IgG_1 (2.1% cytotoxicity).

3.4 | Antitumor Effects of humPMab-117 Against PDPN-Positive Cells in Mouse Xenograft Models

After the inoculation of LN229/PDPN, PC-10, or LN319 at the left flanks of BALB/c nude mice, humPMab-117 or human IgG_1 was intraperitoneally injected into the xenograft-bearing mice on days 8, 15, and 22. The tumor volume was measured on the indicated days. The humPMab-117 administration resulted in a significant reduction in LN229/PDPN xenografts on days 22 ($p < 0.01$) and 25 ($p < 0.01$) compared with that of control human IgG_1 (Figure 6A). In the PC-10 xenograft, a significant reduction was observed on days 22 ($p < 0.01$) and 25 ($p < 0.01$) (Figure 6B). In the LN319 xenograft, a significant reduction was also observed on days 22 ($p < 0.01$) and 25 ($p < 0.01$) (Figure 6C).

In the xenograft weight, humPMab-117 also showed the reduction in LN229/PDPN (36% reduction; $p < 0.01$; Figure 6D), PC-10 (31% reduction; $p < 0.05$; Figure 6E), and LN319 (56% reduction; $p < 0.01$; Figure 6F) compared with control human IgG_1. The resected LN229/PDPN, PC-10, and LN319 tumors on day 25 are shown in each figure. The xenograft-bearing mice on day 25 are

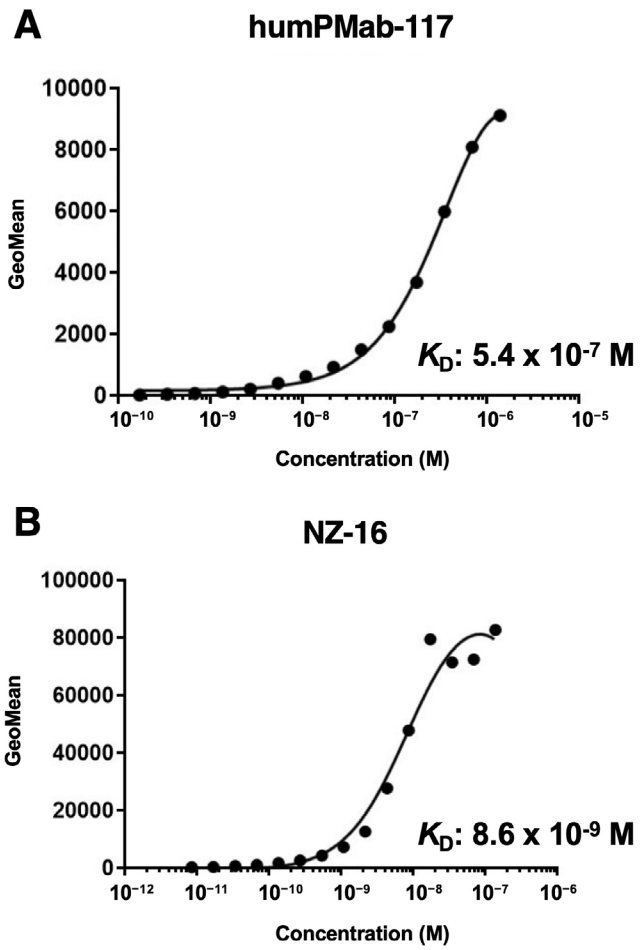

FIGURE 3 | Determination of the binding affinity of humPMab-117 and NZ-16 using flow cytometry. LN229/PDPN cells were suspended in humPMab-117 (A) or NZ-16 (B) at indicated concentrations, followed by treatment with FITC-conjugated anti-human IgG. The SA3800 Cell Analyzer was used to analyze fluorescence data. The dissociation constant (K_D) values were determined using GraphPad Prism 6.

shown in Figure 7A–C and did not lose body weight with the humPMab-117 treatment (Figure 7D–F).

4 | Discussion

This study evaluated the in vitro and in vivo antitumor effects of a novel CasMab against PDPN. The human IgG_1 type PMab-117 (humPMab-117) retained the reactivity to the PDPN-expressing tumor cells but not to normal epithelial cells or kidney podocytes in flow cytometry (Figure 2). Furthermore, humPMab-117 exerted ADCC (Figure 4), CDC (Figure 5), and antitumor effects in LN229/PDPN, PC-10, and LN319 xenografts (Figure 6).

Several preclinical studies have evaluated the antitumor activities of humanized or chimeric anti-PDPN mAbs. The anti-PDPN mAb NZ-1 (a non-CasMab, rat IgG_{2a}) recognizes the PLAG2/3 domain, has a neutralizing activity to the PDPN–CLEC-2 interaction, and inhibits PDPN-induced platelet aggregation and hematogenous lung metastasis [37, 38]. NZ-16, a rat-human chimeric anti-PDPN mAb derived from NZ-1, was developed for alpha-radioimmunotherapy. ^{225}Ac-labeled NZ-16 showed antitumor efficacy against human malignant pleural mesothelioma xenografts and prolonged survival without apparent adverse effect [36].

Another non-CasMab, PG4D2, recognizes the PLD of PDPN and possesses neutralizing activity against the PDPN–CLEC-2 interaction and platelet aggregation [11]. The humanized PG4D2 (AP201) is a human IgG_4 mAb, which does not have ADCC and CDC activity. Nevertheless, AP201 suppressed not only osteosarcoma hematogenous lung metastasis but also xenograft growth [39]. The authors proposed the possibility that platelet-derived growth factors from activated platelets support the osteosarcoma proliferation, which AP201 inhibits. PMab-117 also recognizes the PLD of PDPN [7] and humPMab-117 (human IgG_1) exerted ADCC and CDC activity against PDPN-expressing tumors (Figures 4 and 5). Therefore, it is worthwhile to investigate

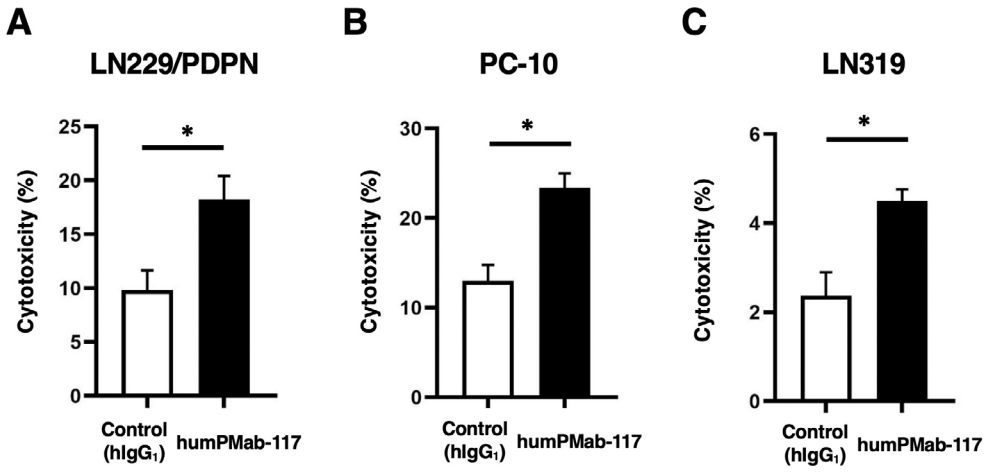

FIGURE 4 | ADCC activity by humPMab-117 against PDPN-positive cells. The target cells labeled with Calcein AM (LN229/PDPN, PC-10, and LN319) were incubated with human NK cells in the presence of humPMab-117 or control human IgG_1 ($hIgG_1$). The ADCC activities against LN229/PDPN (A), PC-10 (B), and LN319 (C) cells were determined by the calcein release. Values are shown as the mean ± SEM. Asterisks indicate statistical significance (*$p < 0.05$; two-tailed unpaired t test).

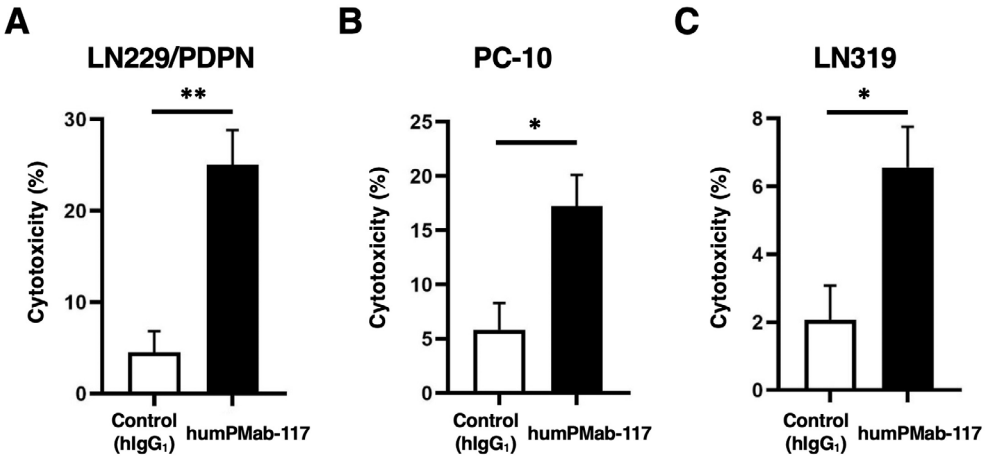

FIGURE 5 | CDC activity by humPMab-117 against PDPN-positive cells. The target cells labeled with Calcein AM (LN229/PDPN, PC-10, and LN319) were incubated with rabbit complement in the presence of humPMab-117 or control human IgG_1 ($hIgG_1$). The CDC activities against LN229/PDPN (A), PC-10 (B), and LN319 (C) cells were determined by the calcein release. Values are shown as the mean ± SEM. Asterisks indicate statistical significance (**$p < 0.01$ and *$p < 0.05$; two-tailed unpaired t test).

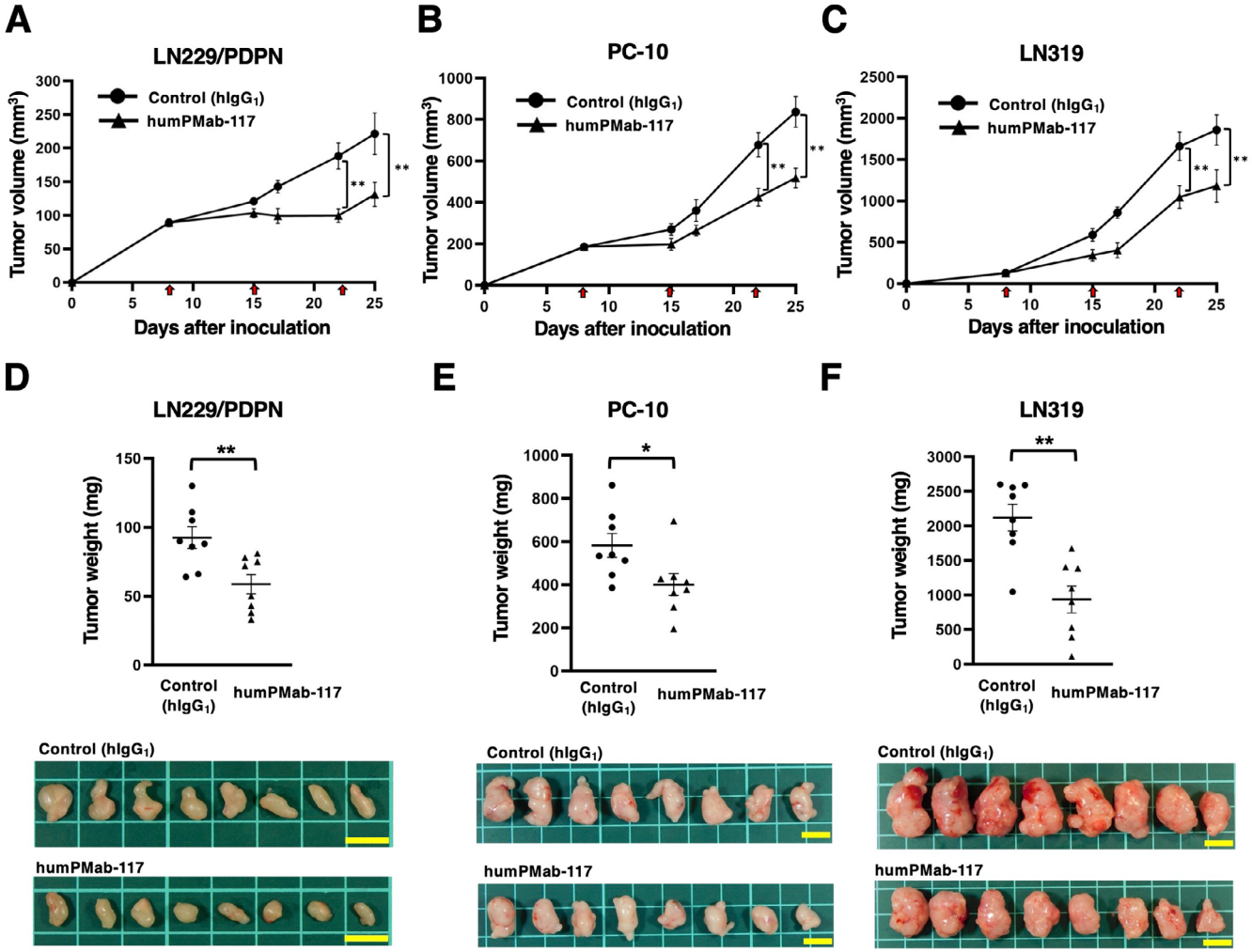

FIGURE 6 | Antitumor activity of humPMab-117 against human tumor xenografts. (A–C) LN229/PDPN (A), PC-10 (B), and LN319 (C) cells were subcutaneously injected into BALB/c nude mice (day 0). humPMab-117 (100 μg) or control human IgG_1 ($hIgG_1$, 100 μg) were intraperitoneally injected into each mouse on days 8, 15, and 22 (arrows). The tumor volume is represented as the mean ± SEM. **$p < 0.01$ (two-way ANOVA with Sidak's post hoc test). (D–F) After cell inoculation, the mice were euthanized on day 25. The tumor weights of LN229/PDPN (D), PC-10 (E), and LN319 (F) xenografts were measured. Values are presented as the mean ± SEM. **$p < 0.01$ and *$p < 0.05$ (two-tailed unpaired t test). Scale bar: 1 cm.

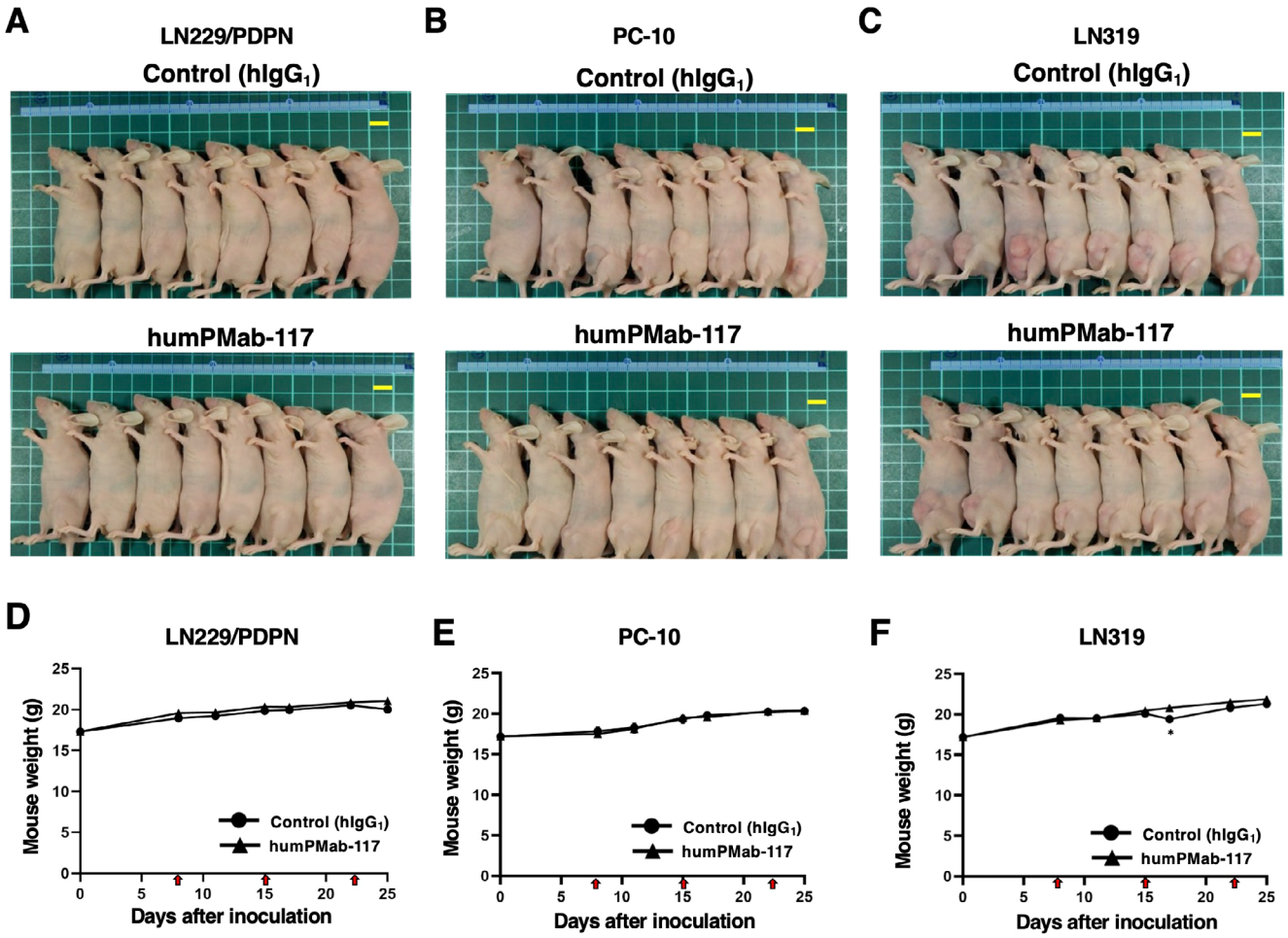

FIGURE 7 | Body appearance and weight in xenografts-bearing mice. (A–C) Body appearance of LN229/PDPN (A), PC-10 (B), and LN319 (C) xenografts-bearing mice treated with humPMab-117 or control human IgG_1 ($hIgG_1$) on day 25. Scale bar: 1 cm. (D–F) Body weights of LN229/PDPN (D), PC-10 (E), and LN319 (F) xenograft-bearing mice treated with control $hIgG_1$ or humPMab-117. The body weight is represented as the mean ± SEM. *$p < 0.05$ (two-way ANOVA with Sidak's post hoc test).

the platelet aggregation-inhibitory effect of humPMab-117 to clarify its contribution to antitumor efficacy.

Although anti-PDPN CasMabs, LpMab-2 and LpMab-23, do not possess neutralizing activity to the PDPN–CLEC-2 interaction, human IgG_1 mAbs, including chLpMab-2, chLpMab-23, and a humanized LpMab-23 (humLpMab-23), exhibited the antitumor effect against human tumor xenograft through ADCC and CDC activity [31, 32, 34]. These results suggest that neutralizing activity is not essential for antitumor efficacy. However, whether these mAbs affect the normal tissue in vivo is a concern. We previously evaluated the toxicity of mouse-human chimeric LpMab-23 (20 mg/kg) against cynomolgus monkeys, and no toxicity was observed [31]. A similar analysis is required to prove the safety of humPMab-117.

The diagnosis to determine the PDPN-positive tumor is also essential for the selection of the patients [40]. LpMab-2, LpMab-23, and PMab-117 recognize different epitopes of PDPN [7]. LpMab-2 and LpMab-23 retain the cancer-specific reactivity in immunohistochemistry [29, 30]. In contrast, PMab-117 is not suitable for immunohistochemistry. PMab-117 did not stain tumor tissues, even if other anti-PDPN mAbs did. This is because it recognizes a structural epitope and does not recognize a denatured epitope in immunohistochemistry. Although the reactivity of humPMab-117 was much weaker than NZ-16 in flow cytometry (Figure 2), humPMab-117 demonstrated significant antitumor activities (Figure 6). The humPMab-117 may recognize a part of the cancer-specific aberrant-structured PDPN. In the anti-HER2 CasMab (H_2Mab-214) case, a reduced condition stimulated the exposure of the cancer-specific HER2 epitope, which enhanced the recognition by H_2Mab-214 [41]. Further studies are essential to clarify the mechanism of recognition by humPMab-117, which could contribute to developing a strategy to promote the exposure of the cancer-specific epitope of PDPN.

As shown in Figure 3, humPMab-117 has approximately 60-fold lower affinity (K_D: 5.4×10^{-7} M) than NZ-16 (K_D: 8.6×10^{-9} M). The K_D values of LpMab-2 and chLpMab-23 were previously determined as 5.7×10^{-9} M and 1.2×10^{-8} M, respectively [29, 31]. A study reported the influence of mAbs' affinity on the antigen internalization and the mAbs' penetration in solid tumors. Derivatives of anti-HER2 mAbs, which recognize the same HER2 epitope (K_D values ranging from 2.7×10^{-7} to 5.6×10^{-10} M), were evaluated in in vitro internalization, in vivo retention, and in vivo tumor penetration. The results showed

that lower-affinity antibodies penetrate tumors more effectively when rates of antibody–antigen dissociation are higher than those of antigen internalization. In contrast, high-density, rapidly internalizing antigens subject high-affinity antibodies to greater internalization and degradation, thereby limiting their penetration of tumors [42]. Since PDPN is also subject to internalization when it binds to anti-PDPN mAbs [43], lower-affinity anti-PDPN mAbs may have therapeutic benefit in efficient penetration in tumors.

We are developing the anti-PDPN mAb-DXd (a topoisomerase I inhibitor exatecan derivative) conjugates. We evaluated the cytotoxicity of humPMab-117-DXd, humLpMab-23-DXd, and NZ-27-DXd. NZ-27 is a humanized anti-PDPN mAb (non-CasMab) and humLpMab-23 is another CasMab against PDPN. The K_D values of NZ-27 and humLpMab-23 to PDPN-expressing cells are 1.1×10^{-8} M and 4.7×10^{-9} M, respectively [34, 44]. Therefore, NZ-27 and humLpMab-23 have high affinity compared with that of humPMab-117 (5.4×10^{-7} M). As shown in Figure S1, NZ-27-DXd and humLpMab-23-DXd showed cytotoxicity at 0.4 and 1.6 μg/mL. However, humPMab-117-DXd did not show cytotoxicity at the same concentrations. These results suggest that low-affinity humPMab-117-DXd was not internalized, whereas high-affinity NZ-27-DXd and humLpMab-23-DXd were internalized and showed cytotoxicity. Although we should consider the different epitopes and reactivity among these mAbs, low-affinity humPMab-117 should be used to exert the ADCC and CDC activities.

CAR-T cell therapy has achieved significant success in the treatment of hematopoietic malignancies [45]. However, the strategy has not been fully translated to solid tumors [46]. The most crucial problem of CAR-T cell therapy against solid tumors is a lack of tumor-specific antigens. Most therapeutic targets, such as epidermal growth factor receptor [47], HER2 [48], and MUC1 [49] are expressed on normal cells, which leads to on-target off-tumor toxicity due to the targeting of normal cells. Since the dosage of CAR-T cells is limited, the reactivity of CAR to normal cells should be minimized. In that sense, our CasMabs against PDPN are suitable for CAR selection. The humanized NZ-1 and LpMab-2-based CAR-T have been evaluated in preclinical models and showed significant antitumor efficacy [50, 51].

As mentioned above, three anti-PDPN CasMabs have different binding affinities ranging from 10^{-7} to 10^{-9} M. Recently, low affinity and avidity CAR-T cell therapy have exhibited enhanced cytotoxicity [52–54], elevated expansion [53, 55], better trafficking [52], and increased selectivity [54]. Furthermore, low affinity and avidity CAR-T cells have been shown to decrease exhaustion [56] and mitigate trogocytosis [55, 57]. It is necessary to explore the cancer-specific reactivity of PMab-117 single-chain Fv for CAR-T cell therapy. It is essential to compare the antitumor activity of three cancer-specific anti-PDPN CAR-T therapies in the future.

Author Contributions

Tomohiro Tanaka: funding acquisition, investigation. **Hiroyuki Suzuki:** funding acquisition, investigation, writing – original draft. **Tomokazu Ohishi:** investigation. **Manabu Kawada:** investigation. **Mika K. Kaneko:** conceptualization. **Yukinari Kato:** conceptualization, funding acquisition, project administration, writing – review and editing.

Ethics Statement

The Animal Ethics Committee of the Institute of Microbial Chemistry approved animal experiments (approval No. 2024-076).

Consent

The authors have nothing to report.

Conflicts of Interest

The authors declare no conflicts of interest.

References

1. S. Paul, M. F. Konig, D. M. Pardoll, et al., "Cancer Therapy With Antibodies," *Nature Reviews. Cancer* 24 (2024): 399–426.

2. M. K. Kaneko, H. Suzuki, and Y. Kato, "Establishment of a Novel Cancer-Specific Anti-HER2 Monoclonal Antibody H(2)Mab-250/H(2) CasMab-2 for Breast Cancers," *Monoclonal Antibodies in Immunodiagnosis and Immunotherapy* 43 (2024): 35–43.

3. M. K. Kaneko, H. Suzuki, T. Ohishi, et al., "Antitumor Activities of a Humanized Cancer-Specific Anti-HER2 Monoclonal Antibody, humH(2)Mab-250 in Human Breast Cancer Xenografts," *International Journal of Molecular Sciences* 26 (2025): 1079.

4. H. Suzuki, T. Ohishi, T. Tanaka, M. K. Kaneko, and Y. Kato, "Anti-HER2 Cancer-Specific mAb, H(2)Mab-250-hG(1), Possesses Higher Complement-Dependent Cytotoxicity Than Trastuzumab," *International Journal of Molecular Sciences* 25 (2024): 8386.

5. M. K. Kaneko, H. Suzuki, T. Ohishi, T. Nakamura, T. Tanaka, and Y. Kato, "A Cancer-Specific Monoclonal Antibody Against HER2 Exerts Antitumor Activities in Human Breast Cancer Xenograft Models," *International Journal of Molecular Sciences* 25 (2024): 1941.

6. M. Hosking, S. Shirinbak, K. Omilusik, et al., "268 Development of FT825/ONO-8250: An Off-The-Shelf CAR-T Cell With Preferential HER2 Targeting and Engineered to Enable Multi-Antigen Targeting, Improve Trafficking, and Overcome Immunosuppression," *Journal for ImmunoTherapy of Cancer* 11 (2023): A307.

7. H. Suzuki, M. K. Kaneko, and Y. Kato, "Roles of Podoplanin in Malignant Progression of Tumor," *Cells* 11, no. 3 (2022): 575, https://doi.org/10.3390/cells11030575.

8. M. Quintanilla, L. Montero-Montero, J. Renart, and E. Martín-Villar, "Podoplanin in Inflammation and Cancer," *International Journal of Molecular Sciences* 20 (2019): 707.

9. Y. Kato, N. Fujita, A. Kunita, et al., "Molecular Identification of Aggrus/T1alpha as a Platelet Aggregation-Inducing Factor Expressed in Colorectal Tumors," *Journal of Biological Chemistry* 278 (2003): 51599–51605.

10. M. K. Kaneko, Y. Kato, A. Kameyama, et al., "Functional Glycosylation of Human Podoplanin: Glycan Structure of Platelet Aggregation-Inducing Factor," *FEBS Letters* 581 (2007): 331–336.

11. T. Sekiguchi, A. Takemoto, S. Takagi, et al., "Targeting a Novel Domain in Podoplanin for Inhibiting Platelet-Mediated Tumor Metastasis," *Oncotarget* 7 (2016): 3934–3946.

12. P. Pandya, J. L. Orgaz, and V. Sanz-Moreno, "Modes of Invasion During Tumour Dissemination," *Molecular Oncology* 11 (2017): 5–27.

13. A. W. Lambert and R. A. Weinberg, "Linking EMT Programmes to Normal and Neoplastic Epithelial Stem Cells," *Nature Reviews. Cancer* 21 (2021): 325–338.

14. J. L. Astarita, S. E. Acton, and S. J. Turley, "Podoplanin: Emerging Functions in Development, the Immune System, and Cancer," *Frontiers in Immunology* 3 (2012): 283.

15. A. Wicki, F. Lehembre, N. Wick, B. Hantusch, D. Kerjaschki, and G. Christofori, "Tumor Invasion in the Absence of Epithelial-Mesenchymal Transition: Podoplanin-Mediated Remodeling of the Actin Cytoskeleton," *Cancer Cell* 9 (2006): 261–272.

16. C. M. de Winde, S. L. George, E. Crosas-Molist, et al., "Podoplanin Drives Dedifferentiation and Amoeboid Invasion of Melanoma," *iScience* 24 (2021): 102976.

17. E. Martín-Villar, D. Megías, S. Castel, M. M. Yurrita, S. Vilaró, and M. Quintanilla, "Podoplanin Binds ERM Proteins to Activate RhoA and Promote Epithelial-Mesenchymal Transition," *Journal of Cell Science* 119 (2006): 4541–4553.

18. A. Pecora, J. Laprise, M. Dahmene, and M. Laurin, "Skin Cancers and the Contribution of Rho GTPase Signaling Networks to Their Progression," *Cancers (Basel)* 13 (2021): 4362, https://pubmed.ncbi.nlm.nih.gov/34503171/.

19. Z. Zhang, M. Liu, and Y. Zheng, "Role of Rho GTPases in Stem Cell Regulation," *Biochemical Society Transactions* 49 (2021): 2941–2955.

20. Y. Y. Li, C. X. Zhou, and Y. Gao, "Podoplanin Promotes the Invasion of Oral Squamous Cell Carcinoma in Coordination With MT1-MMP and Rho GTPases," *American Journal of Cancer Research* 5 (2015): 514–529.

21. E. Martín-Villar, B. Fernández-Muñoz, M. Parsons, et al., "Podoplanin Associates With CD44 to Promote Directional Cell Migration," *Molecular Biology of the Cell* 21 (2010): 4387–4399.

22. G. Friedman, O. Levi-Galibov, E. David, et al., "Cancer-Associated Fibroblast Compositions Change With Breast Cancer Progression Linking the Ratio of S100A4(+) and PDPN(+) CAFs to Clinical Outcome," *Nature Cancer* 1 (2020): 692–708.

23. K. Hirayama, H. Kono, Y. Nakata, et al., "Expression of Podoplanin in Stromal Fibroblasts Plays a Pivotal Role in the Prognosis of Patients With Pancreatic Cancer," *Surgery Today* 48 (2018): 110–118.

24. X. Liu, Y. Cao, K. Lv, et al., "Tumor-Infiltrating Podoplanin(+) Cells in Gastric Cancer: Clinical Outcomes and Association With Immune Contexture," *Oncoimmunology* 9 (2020): 1845038.

25. H. Wang, C. Hu, X. Song, et al., "Expression of Podoplanin in Sinonasal Squamous Cell Carcinoma and Its Clinical Significance," *American Journal of Rhinology & Allergy* 34 (2020): 800–809.

26. M. I. Ramirez, G. Millien, A. Hinds, Y. Cao, D. C. Seldin, and M. C. Williams, "T1alpha, a Lung Type I Cell Differentiation Gene, Is Required for Normal Lung Cell Proliferation and Alveolus Formation at Birth," *Developmental Biology* 256 (2003): 61–72.

27. K. Koop, M. Eikmans, M. Wehland, et al., "Selective Loss of Podoplanin Protein Expression Accompanies Proteinuria and Precedes Alterations in Podocyte Morphology in a Spontaneous Proteinuric Rat Model," *American Journal of Pathology* 173 (2008): 315–326.

28. D. H. Ijpelaar, A. Schulz, K. Koop, et al., "Glomerular Hypertrophy Precedes Albuminuria and Segmental Loss of Podoplanin in Podocytes in Munich-Wistar-Frömter Rats," *American Journal of Physiology-Renal Physiology* 294 (2008): F758–F767.

29. Y. Kato and M. K. Kaneko, "A Cancer-Specific Monoclonal Antibody Recognizes the Aberrantly Glycosylated Podoplanin," *Scientific Reports* 4 (2014): 5924.

30. S. Yamada, S. Ogasawara, M. K. Kaneko, and Y. Kato, "LpMab-23: A Cancer-Specific Monoclonal Antibody Against Human Podoplanin," *Monoclon Antib Immunodiagn Immunother* 36 (2017): 72–76.

31. M. K. Kaneko, T. Nakamura, A. Kunita, et al., "ChLpMab-23: Cancer-Specific Human-Mouse Chimeric Anti-Podoplanin Antibody Exhibits Antitumor Activity via Antibody-Dependent Cellular Cytotoxicity," *Monoclonal Antibodies in Immunodiagnosis and Immunotherapy* 36 (2017): 104–112.

32. M. K. Kaneko, S. Yamada, T. Nakamura, et al., "Antitumor Activity of chLpMab-2, a Human-Mouse Chimeric Cancer-Specific Antihuman Podoplanin Antibody, via Antibody-Dependent Cellular Cytotoxicity," *Cancer Medicine* 6 (2017): 768–777.

33. T. Tanaka, H. Suzuki, T. Ohishi, M. K. Kaneko, and Y. Kato, "A Cancer-Specific Anti-Podoplanin Monoclonal Antibody, PMab-117-mG(2a) Exerts Antitumor Activities in Human Tumor Xenograft Models," *Cells* 13 (2024): 1833, https://pubmed.ncbi.nlm.nih.gov/39594582/.

34. H. Suzuki, T. Ohishi, M. K. Kaneko, and Y. Kato, "A Humanized and Defucosylated Antibody Against Podoplanin (humLpMab-23-f) Exerts Antitumor Activities in Human Lung Cancer and Glioblastoma Xenograft Models," *Cancers (Basel)* 15, no. 20 (2023): 5080, https://doi.org/10.3390/cancers15205080.

35. H. Suzuki, T. Ohishi, T. Tanaka, M. K. Kaneko, and Y. Kato, "A Cancer-Specific Monoclonal Antibody Against Podocalyxin Exerted Antitumor Activities in Pancreatic Cancer Xenografts," *International Journal of Molecular Sciences* 25, no. 1 (2023): 161, https://doi.org/10.3390/ijms25010161.

36. H. Sudo, A. B. Tsuji, A. Sugyo, et al., "Preclinical Evaluation of Podoplanin-Targeted Alpha-Radioimmunotherapy With the Novel Antibody NZ-16 for Malignant Mesothelioma," *Cells* 10, no. 10 (2021): 2503, https://doi.org/10.3390/cells10102503.

37. Y. Kato, M. K. Kaneko, A. Kunita, et al., "Molecular Analysis of the Pathophysiological Binding of the Platelet Aggregation-Inducing Factor Podoplanin to the C-Type Lectin-Like Receptor CLEC-2," *Cancer Science* 99 (2008): 54–61.

38. Y. Kato, M. K. Kaneko, A. Kuno, et al., "Inhibition of Tumor Cell-Induced Platelet Aggregation Using a Novel Anti-Podoplanin Antibody Reacting With Its Platelet-Aggregation-Stimulating Domain," *Biochemical and Biophysical Research Communications* 349 (2006): 1301–1307.

39. A. Takemoto, S. Takagi, T. Ukaji, et al., "Targeting Podoplanin for the Treatment of Osteosarcoma," *Clinical Cancer Research* 28 (2022): 2633–2645.

40. Y. Zhou, L. Tao, J. Qiu, et al., "Tumor Biomarkers for Diagnosis, Prognosis and Targeted Therapy," *Signal Transduction and Targeted Therapy* 9 (2024): 132.

41. T. Arimori, E. Mihara, H. Suzuki, et al., "Locally Misfolded HER2 Expressed on Cancer Cells Is a Promising Target for Development of Cancer-Specific Antibodies," *Structure* 32 (2024): 536–549.e535.

42. S. I. Rudnick, J. Lou, C. C. Shaller, et al., "Influence of Affinity and Antigen Internalization on the Uptake and Penetration of Anti-HER2 Antibodies in Solid Tumors," *Cancer Research* 71 (2011): 2250–2259.

43. Y. Kato, G. Vaidyanathan, M. K. Kaneko, et al., "Evaluation of Anti-Podoplanin Rat Monoclonal Antibody NZ-1 for Targeting Malignant Gliomas," *Nuclear Medicine and Biology* 37 (2010): 785–794.

44. M. K. Kaneko, T. Ohishi, T. Nakamura, et al., "Development of Core-Fucose-Deficient Humanized and Chimeric Anti-Human Podoplanin Antibodies," *Monoclonal Antibodies in Immunodiagnosis and Immunotherapy* 39 (2020): 167–174.

45. "First-Ever CAR T-Cell Therapy Approved in U.S," *Cancer Discovery* 7 (2017): Of1, https://pubmed.ncbi.nlm.nih.gov/28887358/.

46. S. Kakarla and S. Gottschalk, "CAR T Cells for Solid Tumors: Armed and Ready to Go?," *Cancer Journal* 20 (2014): 151–155.

47. K. Feng, Y. Guo, H. Dai, et al., "Chimeric Antigen Receptor-Modified T Cells for the Immunotherapy of Patients With EGFR-Expressing Advanced Relapsed/Refractory Non-Small Cell Lung Cancer," *Science China. Life Sciences* 59 (2016): 468–479.

48. N. Ahmed, V. Brawley, M. Hegde, et al., "HER2-Specific Chimeric Antigen Receptor-Modified Virus-Specific T Cells for Progressive

Glioblastoma: A Phase 1 Dose-Escalation Trial," *JAMA Oncology* 3 (2017): 1094–1101.

49. Z. Mei, K. Zhang, A. K. Lam, et al., "MUC1 as a Target for CAR-T Therapy in Head and Neck Squamous Cell Carinoma," *Cancer Medicine* 9, no. 2 (2020): 640–652, https://doi.org/10.1002/cam4.2733.

50. L. Chalise, A. Kato, M. Ohno, et al., "Efficacy of Cancer-Specific Anti-Podoplanin CAR-T Cells and Oncolytic Herpes Virus G47Δ Combination Therapy Against Glioblastoma," *Molecular Therapy - Oncolytics* 26 (2022): 265–274.

51. S. Shiina, M. Ohno, F. Ohka, et al., "CAR T Cells Targeting Podoplanin Reduce Orthotopic Glioblastomas in Mouse Brains," *Cancer Immunology Research* 4 (2016): 259–268.

52. M. Castellarin, C. Sands, T. Da, et al., "A Rational Mouse Model to Detect On-Target, Off-Tumor CAR T Cell Toxicity. *JCI*," *Insight* 5 (2020): e136012, https://pubmed.ncbi.nlm.nih.gov/32544101/.

53. S. Ghorashian, A. M. Kramer, S. Onuoha, et al., "Enhanced CAR T Cell Expansion and Prolonged Persistence in Pediatric Patients With ALL Treated With a Low-Affinity CD19 CAR," *Nature Medicine* 25 (2019): 1408–1414.

54. S. Arcangeli, M. C. Rotiroti, M. Bardelli, et al., "Balance of Anti-CD123 Chimeric Antigen Receptor Binding Affinity and Density for the Targeting of Acute Myeloid Leukemia," *Molecular Therapy* 25 (2017): 1933–1945.

55. M. L. Olson, E. R. V. Mause, S. V. Radhakrishnan, et al., "Low-Affinity CAR T Cells Exhibit Reduced Trogocytosis, Preventing Rapid Antigen Loss, and Increasing CAR T Cell Expansion," *Leukemia* 36 (2022): 1943–1946.

56. L. D. Caraballo Galva, X. Jiang, M. S. Hussein, et al., "Novel Low-Avidity Glypican-3 Specific CARTs Resist Exhaustion and Mediate Durable Antitumor Effects Against HCC," *Hepatology* 76 (2022): 330–344.

57. M. Hamieh, A. Dobrin, A. Cabriolu, et al., "CAR T Cell Trogocytosis and Cooperative Killing Regulate Tumour Antigen Escape," *Nature* 568 (2019): 112–116.

Supporting Information

Additional supporting information can be found online in the Supporting Information section.